ARCHIVES OF TRANSPORT *ISSN (print):* *0866-9546*
Volume 72, Issue 4, 2024 ***e-ISSN (online):*** *2300-8830*
DOI: *10.61089/aot2024.hgejtx19*

MODELLING AND ANALYSIS OF SELECTED ISSUES OF THE DYNAMICS OF A LAND ROBOT PLATFORM

Zbigniew DZIOPA[1], Andrzej ZUSKA[2], Dariusz WIĘCKOWSKI[3]

[1, 2] *Faculty of Mechatronics and Mechanical Engineering, Kielce University of Technology, Kielce, Poland*

[3] *Institute of Vehicles and Construction Machinery Engineering, Faculty of Automotive and Construction Machinery Engineering, Warsaw University of Technology, Warsaw, Poland*

Abstract:

The research object is a land robot designed to perform special tasks. One of the robot's elements is a six-wheeled platform with independent suspension. The platform allows the robot to move on land and overcome obstacles. Any equipment enabling the robot to perform planned tasks can be mounted on it. If the implementation of the mission requires the platform to move in uneven terrain, external forces are generated resulting from the platform's wheels overcoming uneven road surfaces. Disturbances occurring in the system may negatively affect the measuring and actuating devices mounted on the platform. Actuator devices may also cause additional excitations. This may lead to disruptions in the process of the land robot carrying out its intended work. The aim of the work is to analyse selected dynamics issues with particular emphasis on the modal analysis of the land robot platform and, on this basis, to check the correctness of its design. In order to carry out the tasks set, a physical and mathematical model of the platform was developed. The energy method was used to derive the analytical relationships, which requires the determination of the kinetic energy, the potential energy, the dissipative Rayleigh function and external non-potential forces. A modal analysis was carried out to determine the dynamic parameters of the system and its susceptibility to the generated excitations was determined. The considerations carried out allow for the design of a structure that improves comfort for the actuating devices. Thanks to the developed model, it is possible to select the values and distribution of system parameters in such a way as to exclude the phenomenon of beating and resonance. In the general case, the robot's basic motion is coupled to the disturbances generated in the system. That's why the considerations carried out in this paper are so important, which enable the development of robot platform dynamics that minimize the impacts on the robot's realized fundamental motion.

Keywords: *six-wheeled robot, unmanned ground robot, model*

To cite this article:

Dziopa, Z., Zuska, A., Więckowski, D., (2024). Modelling and analysis of selected platform dynamics issues of a land robot. Archives of Transport, 72(4), 23-41. https://doi.org/10.61089/aot2024.hgejtx19

Contact:
1) zdziopa@tu.kielce.pl [https://orcid.org/0000-0002-9135-6306], 2) a.zuska@tu.kielce.pl [https://orcid.org/0000-0002-9343-9914],
3) dariusz.wieckowski@pw.edu.pl [https://orcid.org/0000-0002-6367-4489] – corresponding author

1. Introduction

The work is devoted to the use of a mobile land robot to perform special tasks. Its undoubted advantage is the ability to perform missions in difficult, uneven terrain without having to expose people to danger resulting from the tasks undertaken. Small dimensions enable transport by air and drop to the target area. This is particularly important if the work is to be performed quickly in an inaccessible, unknown area. The mobility of a small robot and its autonomy is a very important factor for modern activities.

The work discusses a robot that moves on land using a six-wheeled platform with independent suspension. An example is the universal DFRobot 6WD platform presented by BOTLAND, as in Figure 1 (https://botland.com.pl/produkty-wycofane/6626-dfrobot-6wd-6-kolowe-podwozie-robota-z-na-pedem.html 2024.04). A tower equipped with the necessary executive devices is placed on the platform. An example is the IBIS robot presented by PIAP, as in Figure 2 (https://www.antyterroryzm.com/robot-ibis-dla-kolejnych-placowek-stazy-granicznej-w-polsce/ 2024.04). The robot can perform the developed mission autonomously or using remote control.

The aim of the work is to present a model of the dynamics of a land robot platform intended to perform special tasks, and to present a methodology for designing the robot in such a way that its structure, inertia characteristics and the passive vibration isolation used make it possible to reduce the excitations transmitted to the objects on the platform.

The aim of the work is to present a model of the dynamics of a land robot platform intended to perform special tasks. The developed model allows for modal analysis and determination of the dynamic parameters of the system. The obtained dynamic characteristics make it possible to check the susceptibility of the structure to the generated excitations and to predict the occurrence of the beating phenomenon and operation in resonance. The considerations carried out allow for shaping the dynamic characteristics of the system, and thus designing a structure that improves the comfort of the actuator devices.

Fig. 1. The universal DFRobot 6WD platform presented by BOTLAND (https://botland.com.pl/produkty-wycofane/6626-dfrobot-6wd-6-kolowe-podwozie-robota-z-na-pedem.html 2024.04)

Fig. 2. IBIS robot presented by PIAP (https://www.antyterroryzm.com/robot-ibis-dla-kolejnych-placowek-stazy-granicznej-w-polsce/ 2024.04)

Achieving the set goal requires modelling the dynamics of the platform's movement, taking into account the physical phenomena accompanying the operation of the robot (Osiecki&Koruba, 2007), (Dziopa, 2008). The necessary physical model was formulated, and on its basis the equations of motion of the system were derived. Mathematical models were obtained using the variational method based on Lagrange equations of the second type. Having mathematical models, a modal analysis was performed by determining the eigenvalues and the corresponding eigenvectors. Mathematical relationships were also derived to determine the frequency and form of free vibrations. Computer programs have been developed that enable simulation of the system's motion and analysis of the response to the resulting disturbances. The article presents exemplary courses of variability of kinematic quantities characterizing the motion of the model for kinematic forcing with natural frequencies. The basic task of a land robot is to perform a planned mission. The considerations carried out aim to determine the disturbances generated in the system that affect the comfort of the robot's operation

The land robot platform model is formulated in accordance with the principles of analytical mechanics. The movement of the platform is considered in three-dimensional Euclidean space, in the gravitational field and in the earth's atmosphere. Analytical relationships describe a discrete model of a system with a specific number of degrees of freedom.

While developing the spatial model of the robot platform, the following issues were identified and implemented:

1. Physical model(Dziopa, 2008), (Mitschke&Wallentowitz, 2007).
1.1. Inertial elements
1.1.1. The body is perfectly stiff
1.2. Non-inertial elements
1.2.1. Restitution elements
1.2.2. Dissipative elements
1.3. Cartesian orthogonal right-handed reference frames
1.3.1. Galilean system
1.3.2. Non-inertial coordinate systems
1.3.3. Isometric transformations of coordinate systems
1.4. Space
1.4.1. Three-dimensional Euclidean space
1.4.2. Homogeneous gravitational field
1.4.3. Earth's atmosphere
2. Mathematical model (Mitschke&Wallentowitz, 2007), (Misiak, 2017), (Hibbeler,2010), (Trojnacki, 2013), (Howle, 2017), (Gress, 2019).
2.1. Kinematic relationships
2.1.1. Location of inertial elements
2.1.2. Deformation of restoration elements
2.1.3. Static displacements
2.1.4. Speed of inertial elements
2.1.5. The speed of displacement of dissipative elements
2.2. Energy
2.2.1. Kinetic
2.2.2. Potential
2.2.2.1. Resilience
2.2.2.2. Gravitational force fields
2.3. Non-potential forces
2.3.1. Dissipative Rayleigh function
2.4. Equations of motion of the system
2.4.1. Energy method
2.5. Parameters described by functions

Including construction details in the platform model is related to the effectiveness of numerical calculations and substantive necessity assessed in terms of dynamic phenomena. The considered system was reduced to a structural model with a discrete structure, which describes phenomena of the nature of mechanical interactions. The overall motion of the platform is treated as a composite of the basic motion and the basic motion disturbances. The work considers issues arising from the system's response to the generated excitations.

2. Literature review

In recent years, humans have increasingly been replaced by unmanned land robots in performing various dangerous tasks. They replace humans not only in dangerous military missions but, above all, have wide civilian applications in medical rescue, mining, firefighting and so on (Zhang et al., 2021; Ahmed et al., 2020; Shuai et al., 2019; D'Urso et al., 2018; Kayacan et al., 2016).Having robots that can replace people in carrying out particularly dangerous tasks allows for carrying out particularly dangerous missions (Typiak, 2007), (Jarzębowska, 2021), (Spong, 2008).

Based on the way they move, unmanned land robots can be divided into three types: wheeled unmanned robots, tracked unmanned robots and legged

unmanned robots. Unmanned wheeled robots are the most common (Khan et al., 2020). They have the advantage of relatively low energy consumption. Circular land robots include off-road wheeled robots. Their advantage is the ability to maneuver in difficult terrain. The most popular steering system for wheeled terrain robots is one based on the difference in speed of the outer and inner wheels. The lack of a classic steering system is very advantageous, as it reduces their weight. Research on steering systems for wheeled terrain robots has been conducted by (Gupta et al., 2017), (Dogru and Marques, 2019), (Pentzer et al., 2016), (Pace et al., 2017), (Ordonez et al., 2017). Steering these robots, however, is hampered by a complex suspension design.

The essential (basic) components of the design of wheeled land robots include the frame, the drive system, the wheels and suspension, the control and guidance system, the communication system, and the sensor system that ensures smooth control. The design of the frame depends, among other things, on the number of wheels and motors used in the robot (Krishnamurthy, 2008). The effect of the weight of the robot frame on energy consumption was dealt with by (Goris, 2005). The drive systems of wheeled field robots were analyzed by (Siciliano and Khatib, 2008; Shuang et al., 2007). From the point of view of the drive system and suspension, the size of the wheels, the elastic and damping properties of the wheels and the type of tread are very important. In off-road robots, wheels with larger sizes are preferred (Moreland et al., 2012; Skonieczny et al., 2012).

A review of the literature shows that in most cases simulation studies are conducted for dynamic models developed for well-defined assumptions. Many times these are models with only three degrees of freedom. Such limitations make the models very sensitive to perturbations from, for example, varying field (environmental) conditions as demonstrated in this article.

The motion of a robot is a motion composed of fundamental motion and disturbances to the fundamental motion. Forces generated in the robot's system can negatively affect its progressive motion. Therefore, the possibility of shaping the robot's dynamic characteristics makes it possible to provide comfort to the driving system, the progressive motion control system, the drive system, the guidance system and the detector and actuator system (Khan et al., 2020; Mitschke&Wallentowitz, 2007; Klockiewicz Zbyszko, Ślaski Grzegorz 2023, 2024).

The topics of the learned works focus on issues related to fundamental motion, that is, mainly on problems related to the implementation of progressive motion (Tang, S., Yuan, S., Li, X., Zhou, J. 2020;Mokhiamar, O., Amine, S. (2017);Alghanim, M.N., Valavanis, K.P., Rutherford, M.J. 2019), stability and controllability of the autonomous robot (Kang, J., Kim, W., Lee, J., Yi, K. 2010; Goodin, C., et al. 2017;Rivera ZB, De Simone MC, Guida D. 2019).

The actual motion of the robot takes place on the surface, in the gravitational field and in the atmosphere of the earth. It can be treated as complex motion, on which kinematic constraints are imposed, and analyzed in Cartesian coordinate systems. Forces generated in the robot's system can negatively affect both its progressive motion and the objects on the platform under study. The ability to shape the robot's dynamic characteristics makes it possible to provide comfort and safety for the running system, the progressive motion control system, the drive system, the guidance system and the system of detectors and actuators.

There is a lack of information in the literature on the formation of dynamic characteristics of wheeled land robot platforms. Studying the literature in the area of autonomous land robots, no works were found that covered the issues addressed in this paper. It seems to fill the gap that exists in previous research. The primary objective of the analysis carried out was to develop a methodology for designing the robot in such a way that its structure, inertia characteristics and the passive vibration isolation used would enable the reduction of the excitations transmitted to objects on the platform. Using the considerations carried out, the robot can be designed in such a way as to eliminate the need for an active disturbance control system

3. Physical model of the robot

Figure 3 shows the developed physical model of a mobile land robot intended to perform special tasks. The robot consists of a six-wheeled platform with independent suspension on which actuating devices are mounted.

The platform model was assumed in the form of one mass and six deformable elements, as in Figure 3. The platform is a perfectly rigid body with mass m

and moments of inertia I_x,I_z. The platform chassis was modeled as six wheels with independent suspension. The radial compliance characteristics of the tires and their suspension were adopted in the form of linear Kelvin-Voigt models. In order to parameterize the weightless restorative and dissipative elements of the rheological models, the following stiffness and damping coefficients were determined: k_{11} and c_{11} and k_{12} and c_{12} describe suspensions 1 and 2, k_{13} and c_{13} and k_{14} and c_{14} describe suspensions 3 and 4, k_{15} and c_{15} and k_{16} and c_{16} describe suspensions 5 and 6. Geometric characteristics of the platform including parameters necessary to perform the analysis the dynamics of the robot is shown in Figure 3.

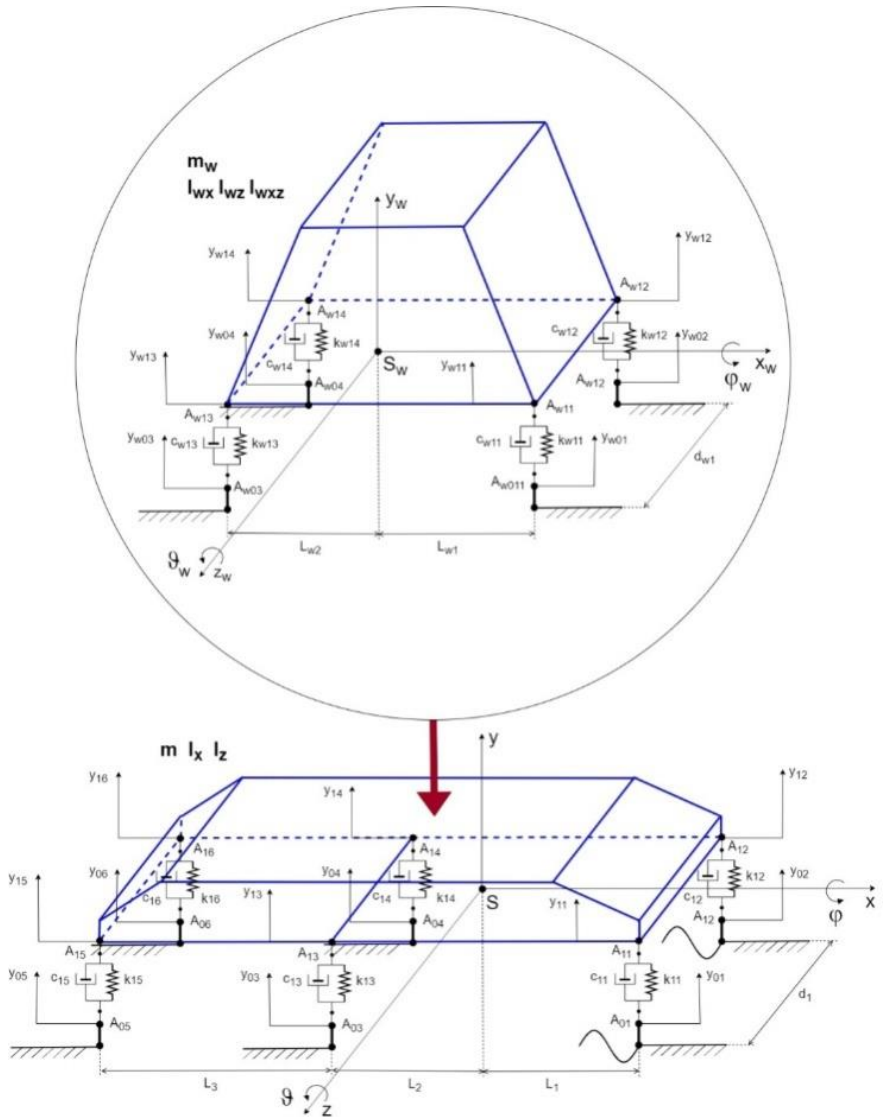

Fig. 3. Physical model of a mobile land robot

The actuators are placed on the platform, modeled as one mass and four deformable elements, as in Figure 3. The actuators are a perfectly rigid body with mass m_{co} and the main central moments of inertia $I_{\xi co}$, $I_{\eta co}$, $I_{\zeta co}$. The characteristics of the flexibility of mounting the actuators on the platform were adopted in the form of linear Kelvin-Voigt models. In order to parameterize the weightless restorative and dissipative elements of the rheological models, the following stiffness and damping coefficients were determined: k_{w11} and c_{w11} with k_{w12} and c_{w12} describe the mounting 1 and 2, k_{w13} and c_{w13} with k_{w14} and c_{w14} describe mounting 3 and 4. The geometric characteristics of the actuating devices, including the parameters necessary to analyze the dynamics of the robot, are shown in Figure 3.

The mounted actuators are equipped with a system that can rotate relative to the platform while performing the task, as in Figure 2. This system is a perfectly rigid body with mass m_{pr} and the main central moments of inertia $I_{\xi pr}$, $I_{\eta pr}$, $I_{\zeta pr}$..

Actuating devices are a time-varying system. The change over time concerns the inertia characteristics of the actuating devices. It depends on the current position of the elements of this system relative to the platform. This applies to relative movements changing the azimuth angle ψ_{wp} and elevation angle ϑ_{wp}. The parameters characterizing the actuating devices are their mass m_w and moments of inertia I_{wx},I_{wz} and the deviation moment I_{wxz}. The inertial parameters of the actuating devices are described by the following relationships:

$$
\begin{aligned}
&m_w = m_{co} + m_{pr},\\
&I_{wx} = \left(I_{\xi co} + I_{\xi pr}cos^2\vartheta_{wp} + I_{\eta pr}sin^2\vartheta_{wp}\right)cos^2\psi_{wp}\\
&\qquad + \left(I_{\zeta co} + I_{\zeta pr}\right)sin^2\psi_{wp},\\
&I_{wz} = \left(I_{\xi co} + I_{\xi pr}cos^2\vartheta_{wp} + I_{\eta pr}sin^2\vartheta_{wp}\right)sin^2\psi_{wp}\\
&\qquad + \left(I_{\zeta co} + I_{\zeta pr}\right)cos^2\psi_{wp},\\
&I_{wxz} = \left(I_{\xi co} + I_{\xi pr}cos^2\vartheta_{wp} + I_{\eta pr}sin^2\vartheta_{wp} - I_{\zeta co}\right.\\
&\qquad \left. - I_{\zeta pr}\right).
\end{aligned}
\tag{1}
$$

The positions of the platform body at any moment of time are determined in Cartesian orthogonal right-handed coordinate systems. The referencesystemsare the followingcoordinatesystems:

a) Earth coordinate system:
   In the case of the mobile land robot under consideration, it can be assumed that the system connected to the earth is a Galilean system.
   $0_g xyz$ - is an inertial, stationary coordinate system related to the road surface. The $0_g x$ and $0_g y$ axes lie in the plane of the road surface, and the $0_g y$ axis points upwards.
b) Coordinate systems defining the movement of the platform:

– $0xyz$ - is a coordinate system moving in basic motion relative to the earth-related coordinate system $0_g xyz$. The condition of parallelism of the corresponding axes osi$0x \,||\, 0_g x$, $0y \,||\, 0_g y$ and $0z \,||\, 0_g z$ is always met. In the adopted model, the basic motion is reduced to a straight-line uniform motion taking place along the $0x$ axis. If the robot moves without any disturbances in its basic motion, at every moment of time point 0 coincides with the center of mass of the platform.
– $Sxyz$ - is a coordinate system that moves, in general, in a translational motion relative to the $0xyz$ coordinate system. The origin of the coordinate system S at every moment of time coincides with the center of mass of the platform. The condition of parallelism of the corresponding axes $Sx \,||\, 0x$, $Sy \,||\, 0y and Sz \,||\, 0z$ is always met. Under the influence of disturbances in the basic motion, the center of mass of the body S moves along the $0y$ axis, which means that in the adopted model the progressive motion is reduced to a straight-line motion.
– $S\xi\eta\zeta$ - is a coordinate system moving, in the general case, in a spherical motion relative to the $Sxyz$. coordinate system. The axes $S\xi$, $S\eta$ and $S\zeta$ are rigidly connected to the body of the platform in such a way that they are its main central axes of inertia. In the general case $d_{11} \neq d_{12}$, $d_{21} \neq d_{22}$ and $d_{31} \neq d_{32}$. Under the influence of disturbances in the basic motion, the body of the platform rotates around the Sz axis in accordance with the change in the tilt angle ϑ and around the Sx axis in accordance with the change in the tilt angle φ, which means that in the adopted model the spherical motion is reduced to two revolutions.

If the robot moves without any disturbances in its basic motion, the coordinate systems $0xyz$, $Sxyz$ and $S\xi\eta\zeta$ coincide with each other at every moment of time. The platform model, as an element of the spatial oscillating system, performs a complex movement relative to the $0xyz$ reference system,

consisting of a rectilinear movement of the center of mass S in accordance with the change in the y coordinate, a rotational movement around the Sz axis in accordance with a change in the inclination angle ϑ, and a rotational movement around the Sx axis in accordance with the change in angle tilt φ.
The number of degrees of freedom resulting from the formulated structure of the platform model describing the disturbances of basic motion in space is three.
Three independent generalized coordinates were adopted to determine the position of the platform at any moment of time:

- y – vertical displacement of the S platform's center of mass.
- φ – rotation angle of the platform around the Sx axis.
- ϑ – rotation angle of the platform around the Sz axis.

4. Excitation from the road surface

While carrying out the planned task, the robot can stop or continue moving along the developed trajectory. In the first case, the system is in a static equilibrium position. The disturbances that arise are the result of the operation of executive devices. In the second case, the system is subjected to external forces resulting from the wheels of the platform overcoming uneven terrain on the road. Also, the change of acceleration as a function of time and the implementation of a curvilinear trajectory may result in additional forces acting on the system. The generated disturbances may negatively affect the implementation of the intended mission by the land robot. When developing the platform model, it was assumed that the radial uniformity of tire stiffness and the balance of the wheels constituting part of the running gear were maintained. An important source of forces acting on the system is the characteristics of the path along which the robot moves. The disturbances that arise are the result of the interaction of the tire with the road surface. When modelling this phenomenon, the radial deformability of the tires was taken into account and enforcement in the form of kinematic relationships determined by the course of vertical displacements of the contact between the wheel and the road surface was assumed. Therefore, the forcing adopted in the considerations is a determined model of the input signals. Four forms of forcing can be used to perform a comprehensive analysis of the dynamic properties of the system.
The first form is a perfectly smooth path, i.e. there is no external forcing on the system. Such a model makes it possible to check whether the robot can perform the planned work under ideal conditions and at what speed of the platform the safety conditions and technical limitations of the actuating devices are exceeded. A positive answer suggests the need to check the system's behaviour in less favourable conditions. The limiting forward speed determined in this way is a measure of the extreme capabilities of the robot in ideally created conditions and is a reference point for further research.
Mathematical model of forcing:

$$y_{01} = 0 \;\; y_{02} = 0 \;\; y_{03} = 0 \;\; y_{04} = 0 \;\; y_{05} = 0 \;\; y_{06} = 0$$

$$\dot{y}_{01} = 0 \;\; \dot{y}_{02} = 0 \;\; \dot{y}_{03} = 0 \;\; \dot{y}_{04} = 0 \;\; \dot{y}_{05} = 0 \;\; \dot{y}_{06} = 0$$

The robot performs basic movement:

$$s = vt$$

The second form is a harmonic excitation with a given amplitude and frequency equal to the natural frequency of the system. Such a model allows checking the system's response to resonance operation and determining the limit value of the excitation amplitude at which unfavorable excitation occurs.
Mathematical model of forcing:

$$\begin{aligned} y_{01} &= A_1 sin(\omega_1 + \alpha_1) \\ \dot{y}_{01} &= A_1\omega_1 cos(\omega_1 + \alpha_1) \\ y_{02} &= A_2 sin(\omega_2 + \alpha_2) \\ \dot{y}_{02} &= A_2\omega_2 cos(\omega_2 + \alpha_2) \\ y_{03} &= A_3 sin(\omega_3 + \alpha_3) \\ \dot{y}_{03} &= A_3\omega_3 cos(\omega_3 + \alpha_3) \\ y_{04} &= A_4 sin(\omega_4 + \alpha_4) \\ \dot{y}_{04} &= A_4\omega_4 cos(\omega_4 + \alpha_4) \\ y_{05} &= A_5 sin(\omega_5 + \alpha_5) \\ \dot{y}_{05} &= A_5\omega_5 cos(\omega_5 + \alpha_5) \\ y_{06} &= A_6 sin(\omega_6 + \alpha_6) \\ \dot{y}_{06} &= A_6\omega_6 cos(\omega_6 + \alpha_6) \end{aligned} \tag{2}$$

The robot does not perform basic movement:

$$v = 0$$

This work presents the system's responses to excitation adopted as a determined model of input signals in the form of harmonic functions.

5. Mathematical model of the platform

Platform motion equations in summation form:

$$\begin{aligned}
&m\ddot{y} + c_{yy}\dot{y} + c_{y\vartheta}\dot{\vartheta} + c_{y\varphi}\dot{\varphi} \\
&\quad + k_{yy}(y + y_{st}) + k_{y\vartheta}(\vartheta + \vartheta_{st}) \\
&\qquad + k_{y\varphi}(\varphi + \varphi_{st}) + mg = \\
&\quad c_{11}\dot{y}_{01} + c_{12}\dot{y}_{02} + c_{13}\dot{y}_{03} + c_{14}\dot{y}_{04} \\
&\qquad + c_{15}\dot{y}_{05} + c_{16}\dot{y}_{06} \\
&\quad + k_{11}y_{01} + k_{12}y_{02} + k_{13}y_{03} + k_{14}y_{04} \\
&\qquad + k_{15}y_{05} + k_{16}y_{06}
\end{aligned}$$

$$\begin{aligned}
&I_z\ddot{\vartheta} + c_{\vartheta y}\dot{y} + c_{\vartheta\vartheta}\dot{\vartheta} + c_{\vartheta\varphi}\dot{\varphi} \\
&\quad + k_{\vartheta y}(y + y_{st}) + k_{\vartheta\vartheta}(\vartheta + \vartheta_{st}) \\
&\qquad + k_{\vartheta\varphi}(\varphi + \varphi_{st}) = \\
&\quad L_1(c_{11}\dot{y}_{01} + c_{12}\dot{y}_{02}) \\
&\qquad - L_2(c_{13}\dot{y}_{03} + c_{14}\dot{y}_{04}) \\
&\qquad - L_3(c_{15}\dot{y}_{05} + c_{16}\dot{y}_{06}) \\
&+ L_1(k_{11}y_{01} + k_{12}y_{02}) - L_2(k_{13}y_{03} + k_{14}y_{04}) \\
&\qquad - L_3(k_{15}y_{05} + k_{16}y_{06})
\end{aligned} \tag{3}$$

$$\begin{aligned}
&I_x\ddot{\varphi} + c_{\varphi y}\dot{y} + c_{\varphi\vartheta}\dot{\vartheta} + c_{\varphi\varphi}\dot{\varphi} \\
&\quad + k_{\varphi y}(y + y_{st}) + k_{\varphi\vartheta}(\vartheta + \vartheta_{st}) \\
&\qquad + k_{\varphi\varphi}(\varphi + \varphi_{st}) = \\
&- c_{11}d_{11}\dot{y}_{01} + c_{12}d_{12}\dot{y}_{02} - c_{13}d_{21}\dot{y}_{03} \\
&\qquad + c_{14}d_{22}\dot{y}_{04} - c_{15}d_{31}\dot{y}_{05} \\
&\qquad + c_{16}d_{32}\dot{y}_{06} \\
&- k_{11}d_{11}y_{01} + k_{12}d_{12}y_{02} - k_{13}d_{21}y_{03} \\
&\qquad + k_{14}d_{22}y_{04} - k_{15}d_{31}y_{05} \\
&\qquad + k_{16}d_{32}y_{06}
\end{aligned}$$

The forcing has a kinematic form determined by the course of vertical displacements of the wheel contact with the road surface.

where:

Equivalent damping tensor:

$$c = \begin{bmatrix} c_{yy} & c_{y\vartheta} & c_{y\varphi} \\ c_{\vartheta y} & c_{\vartheta\vartheta} & c_{\vartheta\varphi} \\ c_{\varphi y} & c_{\varphi\vartheta} & c_{\varphi\varphi} \end{bmatrix} \tag{4}$$

$$\begin{aligned}
c_{yy} &= c_{11} + c_{12} + c_{13} + c_{14} + c_{15} + c_{16} \\
c_{y\vartheta} &= L_1(c_{11} + c_{12}) - L_2(c_{13} + c_{14}) \\
&\quad - L_3(c_{15} + c_{16}) \\
c_{y\varphi} &= -c_{11}d_{11} + c_{12}d_{12} - c_{13}d_{21} + c_{14}d_{22} \\
&\quad - c_{15}d_{31} + c_{16}d_{32} \\
c_{\vartheta y} &= L_1(c_{11} + c_{12}) - L_2(c_{13} + c_{14}) \\
&\quad - L_3(c_{15} + c_{16}) \\
c_{\vartheta\vartheta} &= L_1^2(c_{11} + c_{12}) - L_2^2(c_{13} + c_{14}) \\
&\quad - L_3^2(c_{15} + c_{16}) \\
c_{\vartheta\varphi} &= L_1(c_{12}d_{12} - c_{11}d_{11}) \\
&\quad + L_2(c_{13}d_{21} - c_{14}d_{22}) \\
&\quad + L_3(c_{15}d_{31} - c_{16}d_{32}) \\
c_{\varphi y} &= -c_{11}d_{11} + c_{12}d_{12} - c_{13}d_{21} + c_{14}d_{22} \\
&\quad - c_{15}d_{31} + c_{16}d_{32} \\
c_{\varphi\vartheta} &= L_1(c_{12}d_{12} - c_{11}d_{11}) \\
&\quad + L_2(c_{13}d_{21} - c_{14}d_{22}) \\
&\quad + L_3(c_{15}d_{31} - c_{16}d_{32}) \\
c_{\varphi\varphi} &= c_{11}d_{11}^2 + c_{12}d_{12}^2 + c_{13}d_{21}^2 + c_{14}d_{22}^2 \\
&\quad + c_{15}d_{31}^2 + c_{16}d_{32}^2
\end{aligned}$$

Equivalent stiffness tensor:

$$k = \begin{bmatrix} k_{yy} & k_{y\vartheta} & k_{y\varphi} \\ k_{\vartheta y} & k_{\vartheta\vartheta} & k_{\vartheta\varphi} \\ k_{\varphi y} & k_{\varphi\vartheta} & k_{\varphi\varphi} \end{bmatrix}$$

$$\begin{aligned}
k_{yy} &= k_{11} + k_{12} + k_{13} + k_{14} + k_{15} + k_{16} \\
k_{y\vartheta} &= L_1(k_{11} + k_{12}) - L_2(k_{13} + k_{14}) \\
&\quad - L_3(k_{15} + k_{16}) \\
k_{y\varphi} &= -k_{11}d_{11} + k_{12}d_{12} - k_{13}d_{21} + k_{14}d_{22} \\
&\quad - k_{15}d_{31} + k_{16}d_{32} \\
k_{\vartheta y} &= L_1(k_{11} + k_{12}) - L_2(k_{13} + k_{14}) \\
&\quad - L_3(k_{15} + k_{16}) \\
k_{\vartheta\vartheta} &= L_1^2(k_{11} + k_{12}) - L_2^2(k_{13} + k_{14}) \\
&\quad - L_3^2(k_{15} + k_{16}) \\
k_{\vartheta\varphi} &= L_1(k_{12}d_{12} - k_{11}d_{11}) \\
&\quad + L_2(k_{13}d_{21} - k_{14}d_{22}) \\
&\quad + L_3(k_{15}d_{31} - k_{16}d_{32}) \\
k_{\varphi y} &= -k_{11}d_{11} + k_{12}d_{12} - k_{13}d_{21} + k_{14}d_{22} \\
&\quad - k_{15}d_{31} + k_{16}d_{32} \\
k_{\varphi\vartheta} &= L_1(k_{12}d_{12} - k_{11}d_{11}) \\
&\quad + L_2(k_{13}d_{21} - k_{14}d_{22}) \\
&\quad + L_3(k_{15}d_{31} - k_{16}d_{32}) \\
k_{\varphi\varphi} &= k_{11}d_{11}^2 + k_{12}d_{12}^2 + k_{13}d_{21}^2 + k_{14}d_{22}^2 \\
&\quad + k_{15}d_{31}^2 + k_{16}d_{32}^2
\end{aligned} \tag{5}$$

Platform equilibrium equations in summative form:

$$\begin{aligned} &k_{yy}y_{st} + k_{y\vartheta}\vartheta_{st} + k_{y\varphi}\varphi_{st} + mg = 0 \\ &k_{\vartheta y}y_{st} + k_{\vartheta\vartheta}\vartheta_{st} + k_{\vartheta\varphi}\varphi_{st} = 0 \\ &k_{\varphi y}y_{st} + k_{\varphi\vartheta}\vartheta_{st} + k_{\varphi\varphi}\varphi_{st} = 0 \end{aligned} \tag{6}$$

6. Platform model analysis

6.1. Analysis I

In order to perform modal analysis I, we reduce the mathematical model of the platform to a conservative and autonomous system.

Eigenvalues

We solve the generalized eigenproblem and, based on the characteristic determinant, derive an age (biquadratic) equation.

$$b_3\omega_0^6 + b_2\omega_0^4 + b_1\omega_0^2 + b_0 = 0 \tag{7}$$

where:

$$\begin{aligned} b_0 &= k_{yy}\left(k_{\vartheta\vartheta}k_{\varphi\varphi} - k_{\vartheta\varphi}k_{\varphi\vartheta}\right) \\ &\quad + k_{y\vartheta}\left(k_{\varphi y}k_{\vartheta\varphi} - k_{\varphi\varphi}k_{\vartheta y}\right) \\ &\quad + k_{y\varphi}\left(k_{\vartheta y}k_{\varphi\vartheta} - k_{\vartheta\vartheta}k_{\varphi y}\right) \\ b_1 &= m\left(k_{\vartheta\vartheta}k_{\varphi\varphi} - k_{\vartheta\varphi}k_{\varphi\vartheta}\right) \\ &\quad + I_x\left(k_{yy}k_{\vartheta\vartheta} - k_{y\vartheta}k_{\vartheta y}\right) \\ &\quad + I_z\left(k_{yy}k_{\varphi\varphi} - k_{y\varphi}k_{\varphi y}\right) \\ b_2 &= mI_xk_{\vartheta\vartheta} + mI_zk_{\varphi\varphi} + I_xI_zk_{yy} \\ b_3 &= mI_xI_z \end{aligned}$$

From the age equation, we determine the eigenvalues of the system, which are the dynamic characteristics of the platform. Their distribution depends on the values of the system parameters. The imaginary roots of the characteristic equation are conjugate in pairs.

$$r_j = \pm i\omega_{0j} \tag{8}$$

Where:

$$\begin{aligned} &j = 1,2,3 \\ &r_{j1} = \ \ i\omega_{0j} \\ &r_{j2} = -i\omega_{0j} \end{aligned}$$

Eigenvectors

In order to determine the eigenvectors of the system for the determined natural frequencies, we formulate special integrals and substitute them into differential equations. After transformations, we obtain two algebraic equations for each frequency, from which we determine the values of the coefficients of the distribution of natural vibration amplitudes.

The special integrals of differential equations forming two complex vectors rotating in opposite directions and formulated for the frequency ω_{0j} have the form:

$$\begin{aligned} y_j &= \frac{1}{2}A_{1j}e^{i(\omega_{0j}t+\alpha_j)} + \frac{1}{2}A_{1j}e^{-i(\omega_{0j}t+\alpha_j)} \\ \vartheta_j &= \frac{1}{2}A_{2j}e^{i(\omega_{0j}t+\alpha_j)} + \frac{1}{2}A_{2j}e^{-i(\omega_{0j}t+\alpha_j)} \\ \varphi_j &= \frac{1}{2}A_{2j}e^{i(\omega_{0j}t+\alpha_j)} + \frac{1}{2}A_{2j}e^{-i(\omega_{0j}t+\alpha_j)} \end{aligned} \tag{9}$$

Algebraic equations from which we determine the coefficients of the distribution of natural vibration amplitudes.

$$\begin{aligned} &\left(k_{yy} - m\omega_{01}^2\right)\mu_{1j} + k_{y\vartheta}\mu_{2j} + k_{y\varphi}\mu_{3j} = 0 \\ &k_{\varphi y}\mu_{1j} + k_{\varphi\vartheta}\mu_{2j} + \left(k_{\varphi\varphi} - I_x\omega_{01}^2\right)\mu_{3j} = 0 \end{aligned} \tag{10}$$

where:

$$\begin{aligned} \mu_{1j} &= \frac{A_{1j}}{A_{1j}} = 1 \\ \mu_{2j} &= \frac{A_{2j}}{A_{1j}}, \\ \mu_{3j} &= \frac{A_{3j}}{A_{1j}} \end{aligned}$$

From algebraic equations we determine the eigenvectors of the system, which are the dynamic characteristics of the platform. Their distribution depends on the values of the system parameters and its structure.

6.2. Analysis II

In order to perform modal analysis II, we reduce the mathematical model of the platform to a non-conservative and autonomous system.

Free vibration frequencies

We solve the generalized free problem and derive an age (biquadratic) equation based on the characteristic determinant.

$$\begin{aligned} b_6s^6 + b_5s^5 + b_4s^4 + b_3s^3 + b_2s^2 + b_1s \\ + b_0 = 0 \end{aligned} \tag{11}$$

where:

$$
\begin{aligned}
b_0 &= k_{yy}\left(k_{\vartheta\vartheta}k_{\varphi\varphi} - k_{\vartheta\varphi}k_{\varphi\vartheta}\right) \\
&\quad + k_{y\vartheta}\left(k_{\varphi y}k_{\vartheta\varphi} - k_{\varphi\varphi}k_{\vartheta y}\right) \\
&\quad + k_{y\varphi}\left(k_{\vartheta y}k_{\varphi\vartheta} - k_{\vartheta\vartheta}k_{\varphi y}\right) \\
b_1 &= c_{yy}\left(k_{\vartheta\vartheta}k_{\varphi\varphi} - k_{\vartheta\varphi}k_{\varphi\vartheta}\right) \\
&\quad + c_{\vartheta\vartheta}\left(k_{yy}k_{\varphi\varphi} - k_{y\varphi}k_{\varphi y}\right) \\
&\quad + c_{\varphi\varphi}\left(k_{yy}k_{\vartheta\vartheta} - k_{y\vartheta}k_{\vartheta y}\right) \\
&\quad + c_{y\vartheta}\left(k_{\varphi y}k_{\vartheta\varphi} - k_{\varphi\varphi}k_{\vartheta y}\right) \\
&\quad + c_{y\varphi}\left(k_{\vartheta y}k_{\varphi\vartheta} - k_{\vartheta\vartheta}k_{\varphi y}\right) \\
&\quad + c_{\vartheta y}\left(k_{y\varphi}k_{\varphi\vartheta} - k_{y\vartheta}k_{\varphi\varphi}\right) \\
&\quad + c_{\vartheta\varphi}\left(k_{y\vartheta}k_{\varphi y} - k_{yy}k_{\vartheta\vartheta}\right) \\
&\quad + c_{\varphi y}\left(k_{y\vartheta}k_{\vartheta\varphi} - k_{y\varphi}k_{\vartheta\vartheta}\right) \\
&\quad + c_{\varphi\vartheta}\left(k_{y\varphi}k_{\vartheta y} - k_{yy}k_{\vartheta\varphi}\right) \\
b_2 &= m\left(k_{\vartheta\vartheta}k_{\varphi\varphi} - k_{\vartheta\varphi}k_{\varphi\vartheta}\right) \\
&\quad + I_x\left(k_{yy}k_{\vartheta\vartheta} - k_{y\vartheta}k_{\vartheta y}\right) \\
&\quad + I_z\left(k_{yy}k_{\varphi\varphi} - k_{y\varphi}k_{\varphi y}\right) \\
&\quad + k_{yy}\left(c_{\vartheta\vartheta}c_{\varphi\varphi} - c_{\vartheta\varphi}c_{\varphi\vartheta}\right) \\
&\quad + k_{\vartheta\vartheta}\left(c_{yy}c_{\varphi\varphi} - c_{y\varphi}c_{\varphi y}\right) \\
&\quad + k_{\varphi\varphi}\left(c_{yy}c_{\vartheta\vartheta} - c_{y\vartheta}c_{\vartheta y}\right) \\
&\quad + k_{y\vartheta}\left(c_{\varphi y}c_{\vartheta\varphi} - c_{\varphi\varphi}c_{\vartheta y}\right) \\
&\quad + k_{y\varphi}\left(c_{\vartheta y}c_{\varphi\vartheta} - c_{\vartheta\vartheta}c_{\varphi y}\right) \\
&\quad + k_{\vartheta y}\left(c_{y\varphi}c_{\varphi\vartheta} - c_{y\vartheta}c_{\varphi\varphi}\right) \\
&\quad + k_{\vartheta\varphi}\left(c_{y\vartheta}c_{\varphi y} - c_{yy}c_{\vartheta\vartheta}\right) \\
&\quad + k_{\varphi y}\left(c_{y\vartheta}c_{\vartheta\varphi} - c_{y\varphi}c_{\vartheta\vartheta}\right) \\
&\quad + k_{\varphi\vartheta}\left(c_{y\varphi}c_{\vartheta y} - c_{yy}c_{\vartheta\varphi}\right) \\
b_3 &= m\left(c_{\vartheta\vartheta}k_{\varphi\varphi} + c_{\varphi\varphi}k_{\vartheta\vartheta} - c_{\vartheta\varphi}k_{\varphi\vartheta} - c_{\varphi\vartheta}k_{\vartheta\varphi}\right) \\
&\quad + I_x\left(c_{yy}k_{\vartheta\vartheta} + c_{\vartheta\vartheta}k_{yy} - c_{y\vartheta}k_{\vartheta y} - c_{\vartheta y}k_{y\vartheta}\right) \\
&\quad + I_z\left(c_{yy}k_{\varphi\varphi} + c_{\varphi\varphi}k_{yy} - c_{y\varphi}k_{\varphi y} - c_{\varphi y}k_{y\varphi}\right) \\
&\quad + c_{yy}\left(c_{\vartheta\vartheta}c_{\varphi\varphi} - c_{\vartheta\varphi}c_{\varphi\vartheta}\right) \\
&\quad + c_{y\vartheta}\left(c_{\varphi y}c_{\vartheta\varphi} - c_{\varphi\varphi}c_{\vartheta y}\right) \\
&\quad + c_{y\varphi}\left(c_{\vartheta y}c_{\varphi\vartheta} - c_{\vartheta\vartheta}c_{\varphi y}\right) \\
b_4 &= mI_xk_{\vartheta\vartheta} + mI_zk_{\varphi\varphi} + I_xI_zk_{yy} \\
&\quad + m\left(c_{\vartheta\vartheta}c_{\varphi\varphi} - c_{\vartheta\varphi}c_{\varphi\vartheta}\right) + I_x\left(c_{yy}c_{\vartheta\vartheta} - c_{y\vartheta}c_{\vartheta y}\right) \\
&\quad + I_z\left(c_{yy}c_{\varphi\varphi} - c_{y\varphi}c_{\varphi y}\right) \\
b_5 &= mI_xc_{\vartheta\vartheta} + mI_zc_{\varphi\varphi} + I_xI_zc_{yy} \\
b_6 &= mI_xI_z
\end{aligned}
$$

From the age equation, we determine the free vibration frequencies (natural frequencies) of the system, which are the dynamic characteristics of the platform. Their distribution depends on the values of the system parameters. Roots of the characteristic equation:

$$s_j = s_{j1} \;\; and \;\; s_j = s_{j2} \tag{12}$$

where:

$j = 1,2,3$

Case I – subcritical damping I

The complex roots of the characteristic equation are pairwise conjugate.

$$
\begin{aligned}
s_{j1} &= -h_j + i\omega_{*j} \\
s_{j2} &= -h_j - i\omega_{*j}
\end{aligned} \tag{13}
$$

where:

$$\omega_{*j} = \sqrt{\omega_{0j}^2 - h_j^2} \qquad \omega_{0j} > h_j$$

Case II – critical damping

The real roots of the characteristic equation are double, equal and negative.

$$s_{j1} = s_{j2}$$

Case III – supercritical damping

The real roots of the characteristic equation are unequal and negative.

$$s_{j1} \neq s_{j2}$$

Forms of free vibrations

If all six roots of the characteristic equation are complex numbers and form three pairs of conjugate complex roots whose real parts are negative, then the free vibration mode coefficients can be determined. In order to determine the mode coefficients of the free vibrations of the system, we formulate special integrals for the determined free vibrations and substitute them into the differential equations. After transformations, we obtain two algebraic equations for each frequency, from which we determine the values of the distribution coefficients of free vibration amplitudes.

The special integrals of differential equations forming two complex vectors rotating in opposite directions and formulated for the frequency ω_{*j} have the form:

$$
\begin{aligned}
y_j &= \frac{1}{2}A_{1j}e^{-h_j t+i(\omega_{*j}t+\alpha_j)} \\
&\quad + \frac{1}{2}A_{1j}e^{-h_j t-i(\omega_{*j}t+\alpha_j)} \\
\vartheta_j &= \frac{1}{2}A_{2j}e^{-h_j t+i(\omega_{*j}t+\alpha_j)} \\
&\quad + \frac{1}{2}A_{2j}e^{-h_j t-i(\omega_{*j}t+\alpha_j)} \\
\varphi_j &= \frac{1}{2}A_{2j}e^{-h_j t+i(\omega_{*j}t+\alpha_j)} \\
&\quad + \frac{1}{2}A_{2j}e^{-h_j t-i(\omega_{*j}t+\alpha_j)}
\end{aligned} \tag{14}
$$

Algebraic equations from which we determine the coefficients of the distribution of free vibration amplitudes.

$$
\begin{aligned}
&\left(ms_{j1}^2 + c_{yy}s_{j1} + k_{yy}\right)\mu_{*1j} \\
&\quad + \left(c_{y\vartheta}s_{j1} + k_{y\vartheta}\right)\mu_{*2j} \\
&\quad + \left(c_{y\varphi}s_{j1} + k_{y\varphi}\right)\mu_{*3j} \\
&\quad = 0 s_{j2} = -h_j - i\omega_{*j}
\end{aligned} \tag{15}
$$

$$
\begin{aligned}
&\left(c_{\varphi y}s_{j1} + k_{\varphi y}\right)\mu_{*1j} + \left(c_{\varphi\vartheta}s_{j1} + k_{\varphi\vartheta}\right)\mu_{*2j} \\
&\quad + \left(I_x s_{j1}^2 + c_{\varphi\varphi}s_{j1}\right. \\
&\quad \left. + k_{\varphi\varphi}\right)\mu_{*3j} = 0
\end{aligned}
$$

where:

$$
\mu_{*1j} = \frac{A_{1j}}{A_{1j}} = 1,
$$
$$
\mu_{*2j} = \frac{A_{2j}}{A_{1j}},
$$
$$
\mu_{*3j} = \frac{A_{3j}}{A_{1j}}
$$

From algebraic equations we determine the free vibration mode coefficients of the system, which are the dynamic characteristics of the platform. Their distribution depends on the values of the system parameters and its structure.
For

$$
s_{j1} = -h_j + i\omega_{*j} \tag{16}
$$

we receive

$$
\mu_{*2j} = \left|\mu_{*2j}\right|e^{i\varphi_{2j}}
$$
$$
\mu_{*3j} = \left|\mu_{*3j}\right|e^{i\varphi_{3j}}
$$

For

$$
s_{j2} = -h_j - i\omega_{*j} \tag{17}
$$

we receive

$$
\mu_{*2j} = \left|\mu_{*2j}\right|e^{-i\varphi_{2j}}
$$
$$
\mu_{*3j} = \left|\mu_{*3j}\right|e^{-i\varphi_{3j}}
$$

7. Parameterization and dynamic characteristics of the platform model

7.1. Platform model parameters

Parameters describing inertial elements

$m = 144\ kg$
$I_x = 35\ kgm^2$
$I_z = 110\ kgm^2$

Parameters describing non-inertial elements

$k_{11} = 40000\ N/m$
$k_{12} = 40000\ N/m$
$k_{13} = 50000\ N/m$
$k_{14} = 50000\ N/m$
$k_{15} = 50000N/m$
$k_{16} = 50000\ N/m$
$c_{11} = 80\ Ns/m$
$c_{12} = 80\ Ns/m$
$c_{13} = 80\ Ns/m$
$c_{14} = 80\ Ns/m$
$c_{15} = 80\ Ns/m$
$c_{16} = 80\ Ns/m$

Geometric characteristics

$L = 1.50\ m$
$L_1 = 0.75\ m$
$L_2 = 0.10\ m$
$L_3 = 0.75\ m$
$d = 0.80\ m$
$d_{11} = 0.5\ m$
$d_{12} = 0.3\ m$
$d_{21} = 0.5\ m$
$d_{22} = 0.3\ m$
$d_{31} = 0.5\ m$
$d_{32} = 0.3\ m$
$h = 0.20\ m$

7.2. Modal matrix

The modal matrix contains eigenvectors that depend solely on the structure of the system and its parameters. Therefore, the modal matrix allows for estimation of the dynamic properties of the system. The determined modes of natural

vibrations describe the motion of the system excited by a given frequency of natural vibrations:

$$\mu = \begin{bmatrix} \mu_{11} & \mu_{12} & \mu_{13} \\ \mu_{21} & \mu_{22} & \mu_{23} \\ \mu_{31} & \mu_{32} & \mu_{33} \end{bmatrix}$$

where:

The first form of the platform's natural vibrations (Figure 4).

$\omega_{01} = 46.624917 \left[\frac{\text{rad}}{s}\right]$
$\mu_{11} = 1$
$\mu_{21} = -0{,}2009206$
$\mu_{31} = -1{,}0005757$

The second form of the platform's natural vibrations (Figure 5).

$\omega_{02} = 34.226910 \left[\frac{\text{rad}}{s}\right]$
$\mu_{12} = 1$
$\mu_{22} = -0{,}5221652$
$\mu_{32} = 4{,}4414576$

The third form of the platform's natural vibrations (Figure 6).

$\omega_{03} = 29.809825 \left[\frac{\text{rad}}{s}\right]$
$\mu_{13} = 1$
$\mu_{23} = 5{,}0352577$
$\mu_{33} = 0{,}9341593$

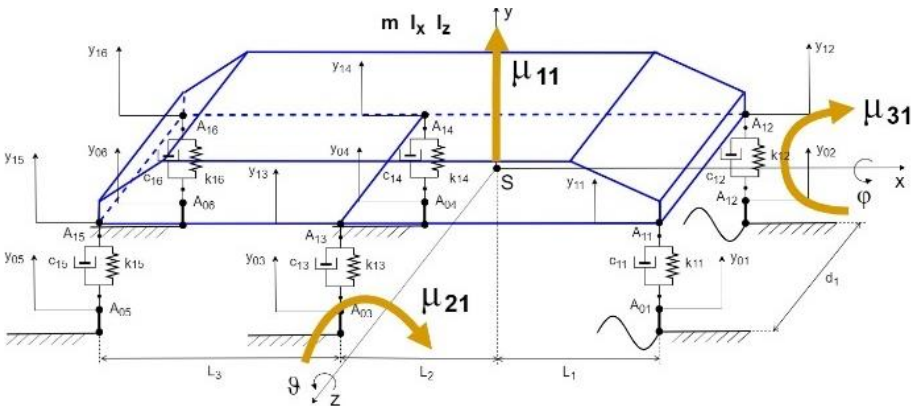

Fig. 4. The first form of the platform's natural vibrations

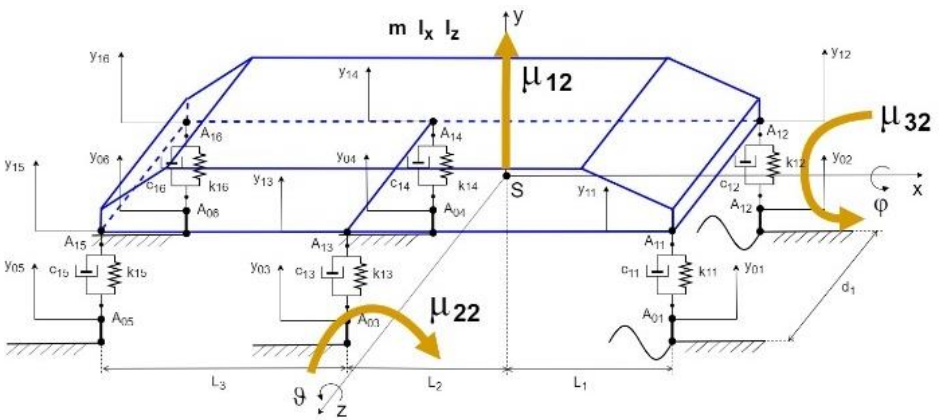

Fig. 5.The second form of the platform's natural vibrations

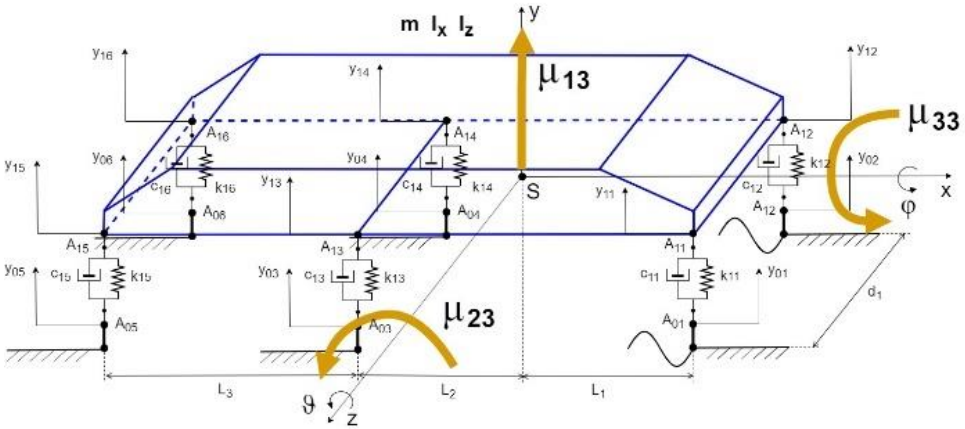

Fig. 6. The third form of the platform's natural vibrations

8. Platform movementsimulation

8.1. Freevibrations

Figure 7 shows the time course of variability of kinematic quantities characterizing the movement of the platform in the case of a non-conservative model, these are y, ϑ, φ and $\dot{y}, \dot{\vartheta}, \dot{\varphi}$.

The introduction of damping reduces vibrations and reduces the rumble phenomenon. The rumbling phenomenon is clearly visible in the variation of the tilt angle φ.

8.2. Forcedvibrations

Figures 8, 9, 10 present the responses of the non-conservative system to the forcing adopted as a determined model of input signals in the form of harmonic functions. The time courses of variability of kinematic quantities characterizing the platform's movement are shown, these are y, ϑ, φ and $\dot{y}, \dot{\vartheta}, \dot{\varphi}$.

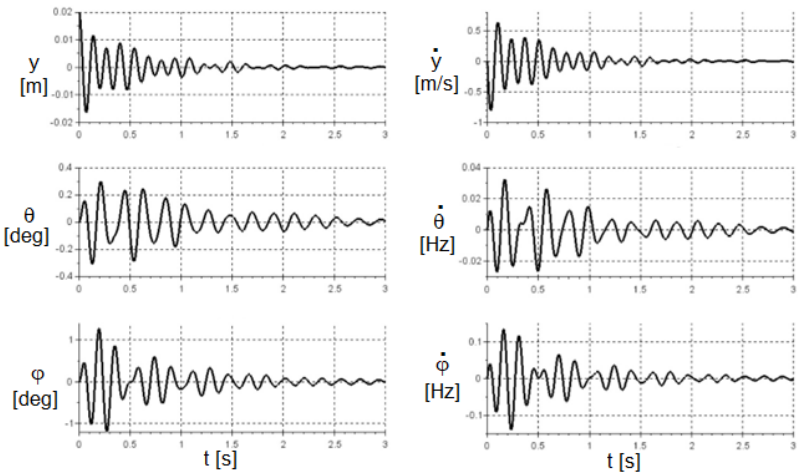

Fig. 7. The course of displacement and velocity variability in vertical movement, pitch and roll

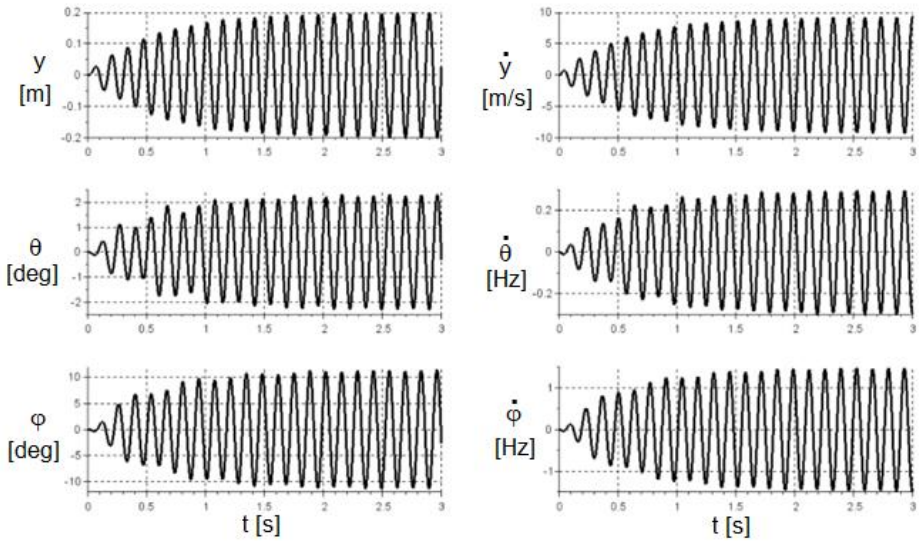

Fig. 8. The course of displacement and velocity variability in vertical movement, inclination and tilting of the platform

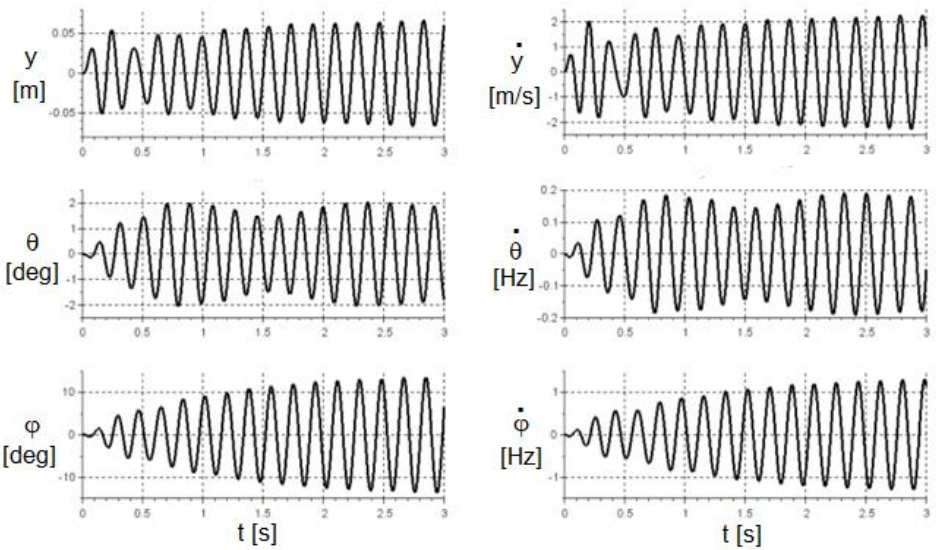

Fig. 9. The course of displacement and velocity variability in vertical movement, inclination and tilting of the platform

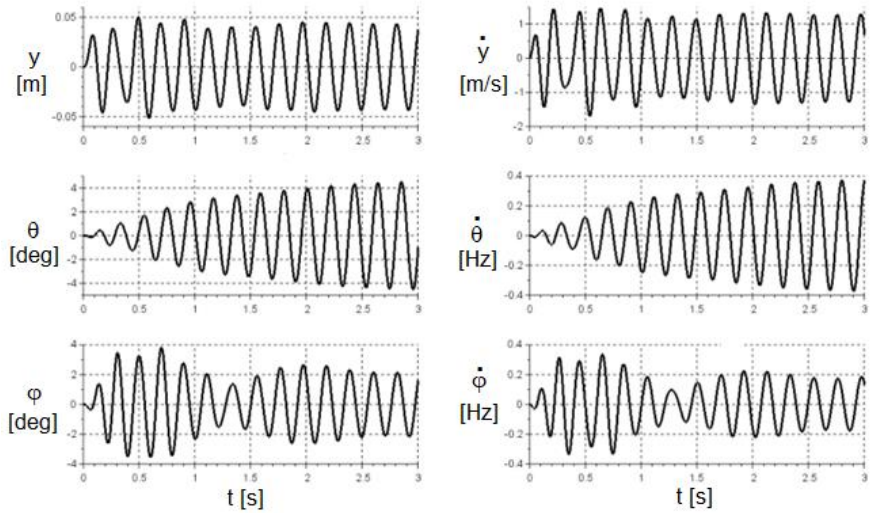

Fig. 10. The course of variability of displacement and speed in vertical movement, tilting and tilting of the platform

System responses for the excitation frequency corresponding to the first mode of natural vibrations

$$\omega_{01} = 46.624917 \left[\frac{\text{rad}}{s}\right]$$

Excitation at this frequency causes a significant increase in the value of the linear displacement and the tilt angle φ of the platform.

System responses for the excitation frequency corresponding to the second mode of natural vibrations

$$\omega_{02} = 34.226910 \left[\frac{\text{rad}}{s}\right]$$

Excitation at this frequency causes a significant increase in the tilt angle φ of the platform. During the variation of the tilt angle ϑ, a beating phenomenon is slightly visible.

System responses for the excitation frequency corresponding to the third mode of natural vibrations

$$\omega_{03} = 29.809825 \left[\frac{\text{rad}}{s}\right]$$

Excitation at this frequency causes a significant increase in the platform inclination angle ϑ. A beating phenomenon is visible in the course of the variation of the tilt angle φ.

9. Discussion of the obtained results

When developing the robot design, attention should be paid to the dynamic characteristics of the platform. The platform is a carrier on which the actuating devices are mounted. The forces that the platform is subjected to are transferred to the actuating devices. Therefore, their unfavourable characteristics may interfere with the operation of measuring and actuating devices mounted on the platform.

The variations of kinematic quantities characterizing the platform's response to the disturbances presented in this paper indicate the occurrence of the beating phenomenon. This phenomenon has an adverse effect on the behaviour of the system and should be eliminated. Introducing damping does not always give the expected result. This can be observed in the considered model.

Figure 7 shows the course of variability of displacement and speed in vertical movement, inclination and tilting of the platform caused by the forcing resulting from the introduction of a non-zero vertical displacement y. A small value of vertical displacement $y_0 = 0.02\ [m]$, which is the initial condition,

causes angular vibrations. This means a clear coupling of vertical movement with angular movements. The variations of angles as a function of time play an important role in the entire process of the robot implementing the planned mission. The introduction of damping reduces vibrations, but their values suggest the possibility of problems in the case of slightly greater force. Analyzing the obtained responses of the system, it is easy to notice the occurrence of the unfavorable phenomenon of rumbling. It is clearly visible in the variation of the tilt angle φ. Some changes of a beating nature can also be seen in the course of the variability of the inclination angle ϑ. This is due to a small difference in the natural frequency values of approximately 4.4 [rad/s]. Even though the considered system is non-conservative, the time elapsed from its excitation to obtaining the minimum vibration amplitude is of the order of 3 [s]. Excessive forces occurring in the system may therefore lead to ineffective operation of the robot. If the determined dynamic characteristics of the designed platform raise concerns, it is recommended to change its parameters or change their distribution.

Not only the rumble phenomenon may negatively affect the robot's ability to perform planned tasks, but also the forcing of the platform with its natural vibration frequencies. While analysing the dynamics of the system, three natural frequencies of vibrations were determined. When constructing the platform, care should be taken to ensure that the frequency band of the excitation from the road side does not coincide with its natural frequencies. This can be observed in the considered model.

Figures 8, 9 and 10 present the variations of displacement and velocity in vertical movement, inclination and tilting of the platform caused by the forcing adopted as a determined model of the input signals. The developed disturbance is a kinematic excitation and has the form of a harmonic function. The mathematical relationships are described by equations in the fourth form, i.e. they are harmonic excitations with a given amplitude and frequency equal to the natural frequency of the system. Thanks to this, it is possible to check, among other things, the system's sensitivity to resonance. Such an analysis is carried out by introducing excitation frequencies with values corresponding to the natural frequencies. In the study, a modal analysis was performed by determining eigenvalues for each independent variable. Then, a simulation of the non-conservative motion of the developed model was performed, obtaining the system responses for the excitation frequencies corresponding to the first, second and third modes of natural vibrations. The amplitudes of all six harmonic functions were 0.02 [m] and the phases were 0.0 [rad]. This is a case of hitting an obstacle with all wheels at the same time. The phenomenon of resonance is clearly visible in all characteristics presented in Fig. 8, 9 and 10. A small value of the amplitude of signals coming from the road surface causes a very significant increase in the amplitude of kinematic quantities characterizing the movement of the platform. You can also notice clear changes of a beating nature in the course of the variation of the pitch angle ϑ as in Fig. 9 and in the course of the variation of the pitch angle φ as in Fig. 10. Operation of the system in an unfavorable frequency band may lead to unfavorable excitation and, consequently, to interference that prevents the operation of the land robot's actuators.

10. Conclusions

The developed platform model and the interpretation of the obtained dynamic characteristics allow for the formulation of conclusions aimed at adapting the robot's structure to the assumed requirements of its operation. A tool was obtained to conduct basic research of the designed structure in virtual space. The developed numerical algorithms make it possible to determine the properties of the system already at the design stage. The introduced models of forcing (options 1,2,3,4) acting directly on the platform play an important role in the assessment of the designed structure.

When designing a robot platform, pay attention to:

- Development of a physical model based on which the properties of the actual structure can be assessed with sufficient accuracy.
- Conducting a modal analysis, which allows for the determination of the dynamic characteristics of the system and the optimal selection of its parameters.
- Eliminating or at least limiting the unfavourable phenomenon of rumbling by changing and distributing the system parameters, selecting the appropriate value of damping coefficients and modifying its structure.
- Eliminating or at least limiting the unfavourable phenomenon of the system operating in resonance. In order to eliminate such a case, the

obtained parameters of the modal matrix should be outside the range of the frequency band generated by the forcing.
– Effect of baseline motion perturbation on the realization of progressive motion using a robot guidance system.

Chapter 9 presents a detailed discussion of the results obtained and the conclusions drawn. Chapter 10 provides basic guidelines to facilitate the design of a robot whose dynamic characteristics will allow the reduction of disturbances due to external forcing. Studying the literature on the class of robots under discussion, no works were found that covered the topics discussed in the presented article. It undoubtedly fills the gap that exists in research.

Further directions of research will oscillate around the implementation of the analyses presented in this article in systems with extensive structure and models that take into account issues of fundamental motion. Specific directions for further research may be related to, among other things:

– The structural development of the platform system, which results from the objects on the platform. These objects are the systems that perform the tasks set for the robot. Determining the dynamic characteristics of such an extended system.
– Ensuring comfort for the objects on the platform by designing a platform with dynamic characteristics that ensure their isolation from external excitations.
– To develop a model of a robot performing complex motion consisting of fundamental motion and fundamental motion disturbances. To check to what extent external excitations can negatively affect the realization of the planned progressive motion and the work the robot performs.
– In the case of the occurrence of excitations whose reduction through the introduction of passive systems is not effective, the development of active or semiactive vibration isolation systems. This may be necessary in the case of higher frequency banded excitations.

References

1. Zhang, H., Liang, H., Tao, X., et al. (2021). Driving Force Distribution and Control for Maneuverability and Stability of a 6WD Skid-Steering EUGV with Independent Drive Motors. *Applied Sciences*, 11(3), 961, 2-21. https://doi.org/10.3390/app11030961
2. Ahmed, M., El-Gindy, M., Lang, H., Omar, M. (2020). Development of Active Rear Axles Steering Controller For 8X8 Combat Vehicle, *SAE Technical Paper*, 2020-01-0174,2020. https://doi.org/10.4271/2020-01-0174
3. Shuai, Z., Li, Ch., Gai, J., et al. (2019). Coordinated motion and powertrain control of a series-parallel hybrid 8 × 8 vehicle with electric wheels. *Mechanical Systems and Signal Processing*, 120, 560-583. https://doi:10.1016/j.ymssp.2018.10.033
4. D'urso, P., El-gindy, M. (2018). Development of control strategies of a multi-wheeled combat vehicle. *International Journal of Automation and Control*, 12.3, 325-360. https://doi:10.1504/IJAAC.2018.10012532
5. Kayacan, E., Ramon, H., Saeys, W. (2016). Robust trajectory tracking error model-based predictive control for unmanned ground vehicles. *IEEE/ASME Transactions on Mechatronics*, 21.2, 806-814. https://doi.org/10.1109/TMECH.2015.2492984
6. Khan, R., Fahat, M. M., Abid, R., Naveed, M. (2021). Comprehensive study of skid-steer wheeled mobile robots: Development and challenges. *Industrial Robot: the international journal of robotics research and application*, 48.1, 142-156. https://doi.org/10.1108/IR-04-2020-0082
7. Gupta, N., Ordonez, C., Collins, E. G. (2017). Dynamically feasible, energy efficient motion planning for skid-steered vehicles. *Autonomous Robots*, 41, 453-471. https://doi.org/10.1007/s10514-016-9550-8
8. Dogru, S., Marques, L. (2019). Power characterization of a skid-steered mobile field robot with an application to headland turn optimization. *Journal of Intelligent & Robotic Systems*, 93, 601-615. https://doi:10.1007/s10846-017-0771-7

9. Pentzer, J., Reichard, K., Brennan, S. (2016). Energy-based path planning for skid-steer vehicles operating in areas with mixed surface types. *In: 2016 American control conference (ACC). IEEE,* 2110-2115. https://doi.org/10.1109/ACC.2016.7525230
10. Pace, J., Harper, M., Ordonez, C., et al. (2017). Experimental verification of distance and energy optimal motion planning on a skid-steered platform. *In: Unmanned Systems Technology XIX. SPIE,* 51-58. http://dx.doi.org/10.1117/12.2262921
11. Ordonez, C., Gupta, N., Reese, B., et al. (2017). Learning of skid-steered kinematic and dynamic models for motion planning. *Robotics and Autonomous Systems*, 95 (2), 207-221. http://dx.doi.org/10.1016/j.robot.2017.05.014
12. Krishnamurthy, D. A. (2008). Modeling and simulation of skid steered robot pioneer 3at.*Florida State University Libraries, Electronic Theses, Treatises and Dissertations*. USA. http://rightsstatements.org/vocab/InC/1.0/
13. Goris, K. (2005). Autonomous mobile robot mechanical design. *Vrije Universiteit Brussel, Engineering Degree Thesis*, Brussels, Belgium. http://mech.vub.ac.be/multibody/final_works/ThesisKristofGoris.pdf
14. Siciliano, B., Khatib, O. (Eds.) (2008). *Springer handbook of robotics.* Berlin: Springer. https://doi:10.1007/978-3-319-32552-1
15. Shuang, G., Cheung, N. C., Cheng, K. W. E., al. (2007). Skid steering in 4-wheel-drive electric vehicle. *In: 2007 7th International Conference on Power Electronics and Drive Systems. IEEE,* 1548-1553. http://dx.doi.org/10.1109/PEDS.2007.4487913
16. Moreland, S., Skonieczny, A., Inotsume, H., Wettergreen, D. (2012). Soil behavior of wheels with grousers for planetary rovers. *In: 2012 IEEE Aerospace Conference*. 1-8. http://dx.doi.org/10.1109/AERO.2012.6187040
17. Skonieczny, K., Moreland, S.J., Wettergreen, D. (2012). grouser spacing equation for determining appropriate geometry of planetary rover wheels. *In: 2012 IEEE/RSJ International Conference on Intelligent Robots and Systems. IEEE,* 5065-5070. http://dx.doi.org/10.1109/IROS.2012.6386203
18. Klockiewicz, Z., Ślaski, G. (2024). The effectiveness of damping for SkyHook control strategy depending on how realistic damper model is. *Vibrations in Physical Systems - 2024*, 35(1). https://doi:10.21008/j.0860-6897.2024.1.20.
19. Klockiewicz, Z., Ślaski, G. (2023). Comparison of Vehicle Suspension Dynamic Responses for Simplified and Advanced Adjustable Damper Models with Friction, Hysteresis and Actuation Delay for Different Comfort-Oriented Control Strategies. *Acta Mechanica et Automatica-2023*, 17(1), 1-15. https://doi:10.2478/ama-2023-0001
20. Mitschke, M., Wallentowitz, H. (2014). *Dynamik der Kraftfahrzeuge. Springer-Verlag*, Berlin-Heidelberg. ISBN 3658050683, 9783658050689.
21. Typiak, A. (2007). Bezzałogowe pojazdy lądowe w zastosowaniach militarnych. *Pomiary Automatyka Robotyka* (Unmanned land vehicles in military applications. *Measurements Automation Robotics*, Poland). 2/2007. http://www.par.pl/
22. Jarzębowska E. (2021). Dynamika i sterowanie układami mechanicznymi. (Dynamics and control of mechanical systems). PWN, Warszawa 2021, Poland. ISBN: 9788301219536.
23. Spong M.W., Vidyasagar M. (2024). Robot Dynamics and Control. *Wiley India PvtLtd* 2008. ISBN: 978-0-471-61243-8.
24. https://botland.com.pl/produkty-wycofane/6626-dfrobot-6wd-6-kolowe-podwozie-robota-z-napedem.html (Access from 2024.04.01).
25. https://www.antyterroryzm.com/robot-ibis-dla-kolejnych-placowek-stazy-granicznej-w-polsce/ (Access from 2024.04.01).
26. Osiecki J., Koruba Z. (2007). Elementy mechaniki zaawansowanej. *Politechnika Świętokrzyska, Podręcznik akademicki* (Elements of advanced mechanics. Kielce University of Technology. Academic textbook). Kielce. *2007*. http://katalog.tu.kielce.pl/EOSWeb/OPAC/Search/AdvancedSearch.asp
27. Dziopa, Z. (2008). Modelowanie i badanie dynamicznych właściwości samobieżnych przeciwlotniczych zestawów rakietowych (Modeling and testing of dynamic properties of self-propelled anti-aircraft

missile systems). *Monografie, Studia, Rozprawy M9*, Kielce University of Technology, Kielce, 2008, PL ISSN 1897-2691.
28. Misiak J. (2017). Mechanika techniczna, tom II Kinematyka i Dynamika. (Technical mechanics, volume II Kinematics and Dynamics.). *Wydawnictwo Naukowe PWN*, Warszawa 2017. Poland. ISBN/ISSN: 978-83-01-19113-9.
29. Hibbeler, R.C. (2010). Engineering mechanics, Dynamics, 12th edition. *Published by Pearson Prentice Hall*. Printed in the United States of America. ISBN -10: 0-13-60779 1-9.
30. Trojnacki, M. (2013). Modelowanie dynamiki mobilnych robotów kołowych. (Modeling the dynamics of mobile wheeled robots.). Monografia, Oficyna Wydawnicza PIAP, Warszawa 2013. Poland. ISSN 0033-2097.
31. Howle D., Krayterman D., Pritchett J.E., Sorenson R. (2017). Validating a Finite Element Model of a Structure Subjected to Mine Blast with Experimental Modal Analysis [Research Report].*ARLTR-8224; Army Research Laboratory*: Aberdeen, USA, 2017. AD1042331. https://apps.dtic.mil/sti/pdfs/AD1042331.pdf
32. Gres, S., Andersen, P., Hoen, C., Damkilde, L. (2018). Orthogonal projection-based harmonic signal removal for operating modal analysis. *W: Structural Health Monitoring, Photogrammetry & DIC, Volume 6: Proceedings of the 36th IMAC, A Conference and Exposition on Structural Dynamics 2018. Springer International Publishing*. 9-21. https://doi:10.1007/978-3-319-74476-6_2
33. Tang, S., Yuan, S., Li, X. and Zhou, J. (2020). Dynamic modeling and experimental validation of skid-steered wheeled vehicles with low-pressure pneumatic tires on soft terrain. *Proceedings of the Institution of Mechanical Engineers*. 840–856. https://doi.org/10.1177/0954407019847302
34. Mokhiamar, O., Amine, S. (2017). Lateral motion control of skid steering vehicles using the full drive-by-wire system. *Alexandria Engineering Journal*, 56(4). 383-394. https://doi.org/10.1016/j.aej.2017.03.024
35. Alghanim, M. N., Valavanis, K. P., Rutherford, M. J. (2019). Modeling, control, and wheel-terrain interaction dynamics of the UGV argo J5. *2019 18th European Control Conference (ECC), IEEE*, 1116-1123. https://doi.org/10.23919/ECC.2019.8796270
36. Kang, J., Kim, W., Lee, J. Yi, K. (2010). Skid steering-Based control of a robotic vehicle with six in-wheel drives. *Proceedings of the Institution of Mechanical Engineers, Part D: Journal of Automobile Engineering*, 224, 1369-1391. https://doi.org/10.1243/09544070JAUTO1405
37. Goodin, C., Carrilllo J. T., McInnis, D. P., et al. (2017). Unmanned ground vehicle simulation with the virtual autonomous navigation environment. *2017 International Conference on Military Technologies (ICMT), IEEE*, 160-165. https://doi.org/10.1109/MILTECHS.2017.7988748
38. Rivera, Z. B., De Simone, M.C., Guida, D. (2019). Unmanned Ground Vehicle Modelling in Gazebo/ROS-Based Environments. *Machines*, 7(2):42, 2-21. https://doi.org/10.3390/machines7020042